frontiers in Earth Science

ORIGINAL RESEARCH
published: 11 April 2019
doi: 10.3389/feart.2019.00074

# Pacific Southwest United States Holocene Droughts and Pluvials Inferred From Sediment $\delta^{18}O_{(calcite)}$ and Grain Size Data (Lake Elsinore, California)

*Matthew Edward Christopher Kirby[1]*, William Paul Patterson[2], Matthew Lachniet[3], James A. Noblet[4], Michael A. Anderson[5], Kevin Nichols[6] and Judith Avila[1]*

*[1] Department of Geological Sciences, California State University, Fullerton, Fullerton, CA, United States, [2] Department of Geological Sciences, University of Saskatchewan, Saskatoon, SK, Canada, [3] Department of Geoscience, University of Nevada, Las Vegas, Las Vegas, NV, United States, [4] Department of Chemistry and Biochemistry, California State University, San Bernardino, San Bernardino, CA, United States, [5] Department of Environmental Sciences, University of California, Riverside, Riverside, CA, United States, [6] Department of Mathematics, California State University, Fullerton, Fullerton, CA, United States*

OPEN ACCESS

**Edited by:**
*Lesleigh Anderson, United States Geological Survey, United States*

**Reviewed by:**
*Maarten Blaauw, Queen's University Belfast, United Kingdom*
*Olga Nikolaevna Solomina, Institute of Geography (RAS), Russia*
*Matthew Jones, University of Nottingham, United Kingdom*

***Correspondence:**
*Matthew Edward Christopher Kirby*
*mkirby@fullerton.edu*

**Specialty section:**
*This article was submitted to Quaternary Science, Geomorphology and Paleoenvironment, a section of the journal Frontiers in Earth Science*

**Received:** *24 September 2018*
**Accepted:** *22 March 2019*
**Published:** *11 April 2019*

**Citation:**
*Kirby MEC, Patterson WP, Lachniet M, Noblet JA, Anderson MA, Nichols K and Avila J (2019) Pacific Southwest United States Holocene Droughts and Pluvials Inferred From Sediment $\delta^{18}O_{(calcite)}$ and Grain Size Data (Lake Elsinore, California). Front. Earth Sci. 7:74. doi: 10.3389/feart.2019.00074*

Records of past climate can inform us on the natural range and mechanisms of climate change. In the arid Pacific southwestern United States (PSW), which includes southern California, there exist a variety of Holocene records that can be used to infer past winter conditions (moisture and/or temperature). Holocene records of summer climate, however, are rare from the PSW. In the future, climate changes due to anthropogenic forcing are expected to increase the severity of drought in the already water stressed PSW. Hot droughts are of considerable concern as summer temperatures rise. As a result, understanding how summer conditions changed in the past is critical to understanding future predictions under varied climate forcings. Here, we present a c. 10.9 kcal BP $\delta^{18}O_{(calcite)}$ record from Lake Elsinore, California, interpreted to reflect $\delta^{18}O_{(lake\,water)}$ values as controlled by over-water evaporation from summer-to-early fall. Our results reveal three millennial scale intervals: (1) the highly evaporative Early Holocene (10.55–6.65 kcal BP), (2) the less evaporative Mid-Holocene (6.65–2.65 kcal BP); and (3) the evaporative Late Holocene (2.65–0.55 kcal BP). These results are coupled with an inferred winter precipitation runoff (sand content) record from Kirby et al. (2010). Using these data together, we estimate the duration and severity of centennial-scale Holocene droughts and pluvials (e.g., high $\delta^{18}O_{(calcite)}$ values plus low sand content = drought and vice versa). Furthermore, the coupled $\delta^{18}O_{(calcite)}$ and sand data provide a generalized Holocene lake level history. The most severe, long-lasting droughts (i.e., maximum summer-to-early fall evaporation and minimum winter precipitation runoff) occur in the Early Holocene. Fewer, less severe, and shorter duration droughts occurred during the Mid-Holocene as pluvials became more common. Droughts return with less severity and duration in the Late Holocene. Notably, the Little Ice Age is characterized as the wettest period during the Late Holocene.

**Keywords: Lake Elsinore, isotopes, holocene, evaporation, drought**

## INTRODUCTION

Extracting seasonality from climatic archives is a major challenge in the field of paleoclimatology (Anderson et al., 1987; Leavitt and Long, 1991; Wurster and Patterson, 2001; Miller et al., 2010; Labotka et al., 2016). For success, the archive must, in some way, capture varying seasonal signals through time. Moreover, the seasonal signal must be strong enough for subsequent preservation, extraction, and interpretation. This is easier said than done. In the winter precipitation dominated, Pacific southwestern United States (PSW), for example, most previous Holocene-length work infers some component of past winter hydroclimates, without any significant insight to summer conditions (Enzel and Wells, 1997; McDonald et al., 2003; Wells et al., 2003; Bird and Kirby, 2006; Bird et al., 2010; Kirby et al., 2010, 2012, 2014, 2015; Pigati et al., 2011). This insight includes the highly resolved tree ring records for the PSW, which record predominantly winter precipitation surpluses and deficits (Graumlich, 1993; Hughes and Graumlich, 1996; Meko et al., 2001; Cook et al., 2007, 2014, 2015; Wise, 2010, 2016; Ault et al., 2013; Griffin and Anchukaitis, 2014; St George and Ault, 2014). Nonetheless, the characterization and explanation of Holocene summer climate is important, particularly for the PSW where summer conditions rapidly amplify, or reduce, winter-generated water deficiencies (i.e., drought) (Griffin and Anchukaitis, 2014; Cook et al., 2015; Diffenbaugh et al., 2015; Shukla et al., 2015; Luo et al., 2017). For example, the most recent Californian drought (2012–2015 AD) is attributed generally to changes in temperature rather than simple reductions precipitation; this is sometimes referred to as a "hot drought" (Griffin and Anchukaitis, 2014; Diffenbaugh et al., 2015; Shukla et al., 2015; Luo et al., 2017).

Fortunately, there are a handful of Holocene PSW summer reconstructions from which we can begin to build a story (cf. Metcalfe et al., 2015). For example, paleo-runoff records from a Mojave Desert alluvial fan (Miller et al., 2010) suggest periods of increased summer precipitation (i.e., North American monsoon) in the Mojave region between 14–9 and 6–3 kcal BP (1000s or years before the present, where the present is AD 1950). However, McDonald et al. (2003) attribute these periods to more frequent warm season tropical cyclones rather than monsoonal moisture. Holmgren et al. (2010) use packrat middens from Joshua Tree National Park to infer the post-glacial onset of monsoonal moisture into southeastern CA by 11 kcal BP. There is, however, only one Holocene summer paleotemperature reconstruction from the study region – a July temperature pollen-reconstruction for the San Jacinto Mountains (headwaters to Lake Elsinore) (Wahl, 2002; Ohlwein and Wahl, 2012). In general, this pollen reconstruction shows above-average to average July temperatures for most of the Holocene, excepting a cooling at 2.4 and 0.3–0.2 kcal BP. A closer look reveals a more nuanced signal described in the discussion. In the adjacent San Bernardino Mountains, Bird and Kirby (2006), Bird et al. (2010), and Kirby et al. (2012) argue that enhanced Early Holocene runoff and associated higher lake levels at Dry Lake may reflect an expanded monsoon in response to higher-than-today, summer insolation. Kirby et al. (2005, 2007) proposed a similar mechanism for enhanced runoff into Lake Elsinore during the Early Holocene. However, neither of these lake studies can provide unequivocal evidence for summer climate, only inferred evidence based on suspected climatic forcings (i.e., summer insolation effect).

Combined with an existing reconstruction of historical winter precipitation and runoff from Lake Elsinore, here we re-examine the site's Holocene record using a particularly sensitive lake sediment proxy for arid and semi-arid environment lakes – the oxygen isotopes of endogenic calcite (Leng and Marshall, 2004; Steinman and Abbott, 2013; Dean et al., 2015; Anderson et al., 2016; Horton et al., 2016). The stable oxygen isotopes values ($\delta^{18}O$) of lacustrine endogenic calcite reflect a combination of water temperature and the $\delta^{18}O_{(lake\ water)}$ values during mineral precipitation (e.g., Stuiver, 1970). Lakes located in arid regions, such as Lake Elsinore, often display variations in $\delta^{18}O_{(lake\ water)}$ associated with changing P:E ratios (precipitation : evaporation) more so than lake water temperature changes (Kelts and Talbot, 1990; Li and Ku, 1997; Li et al., 2000; Kirby et al., 2004; Leng and Marshall, 2004; Dean et al., 2015). Rather, the $\delta^{18}O_{(lake\ water)}$ values are primarily controlled by the rate of evaporation and lake source water $\delta^{18}O$ values, including lake water residence time (Kelts and Talbot, 1990; Li and Ku, 1997; Li et al., 2000; Benson et al., 2002; Leng and Marshall, 2004; Dean et al., 2015). Using modern isotopic and hydrologic observations from a lake helps to unravel these complexities (Steinman and Abbott, 2013; Dean et al., 2015). With the supporting modern lake water, the dominant hydroclimatic signal preserved in the $\delta^{18}O_{(calcite)}$ values can be inferred back through time.

In this paper, we use a lacustrine sediment $\delta^{18}O_{(calcite)}$ archive from Lake Elsinore, California to infer centennial to multi-centennial scale changes in Holocene summer-to-early fall $\delta^{18}O_{(lake\ water)}$ values (i.e., period of maximum $CaCO_3$ precipitation). In turn, these changes are interpreted to reflect summer-to-early fall over-water evaporation. Combined with a winter precipitation and runoff history based on sand content (Kirby et al., 2010), we consider the severity and duration of past Holocene droughts and pluvials that also provides a generalized Holocene lake level history. Finally, we compare our results to a pollen-based, July temperature anomaly reconstruction from the San Jacinto Mountains – the headwater catchment area for Lake Elsinore (Wahl, 2002; Ohlwein and Wahl, 2012).

## BACKGROUND

### Study Site and Limnology

Lake Elsinore is the largest natural lake in the PSW (**Figure 1**). This pull-apart basin contains a sediment package of up to 1000 m based on gravimetric studies (Hull, 1990). The lake is polymictic, experiences occasional hypolimnic anoxia, and precipitates epilimnic $CaCO_3$. The highest rates of $CaCO_3$ precipitation occur in the warm summer months, based on sediment trap studies (Anderson, 2001). At Elsinore, $CaCO_3$ precipitation is likely the result of late-spring/summer/early fall algae blooms, their photosynthetic uptake of $CO_2$, and the subsequent change in epilimnic pH, which favors the precipitation of $CaCO_3$ (Anderson, 2001). Warm season, biomediated $CaCO_3$ precipitation in lacustrine environments

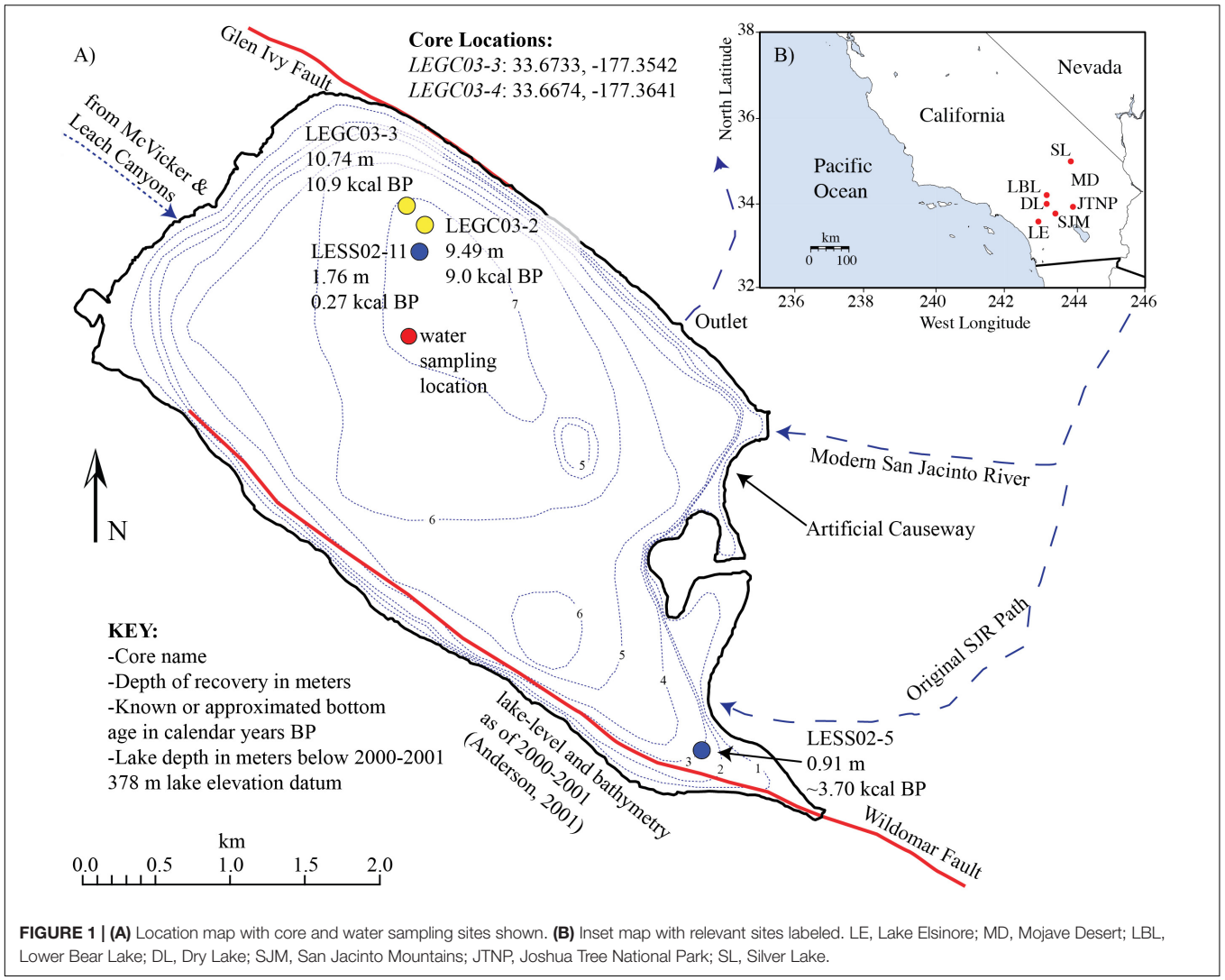


**FIGURE 1 | (A)** Location map with core and water sampling sites shown. **(B)** Inset map with relevant sites labeled. LE, Lake Elsinore; MD, Mojave Desert; LBL, Lower Bear Lake; DL, Dry Lake; SJM, San Jacinto Mountains; JTNP, Joshua Tree National Park; SL, Silver Lake.

is a well-documented phenomenon with proven value for interpreting past lake conditions (Lebo et al., 1994; Anderson et al., 1997; Thompson et al., 1997; Hodell et al., 1998; Mullins, 1998, 2011; Kirby et al., 2002, 2004; Lajewski et al., 2003; Leng and Marshall, 2004). The preservation of warm season precipitated $CaCO_3$ is also favored by a warmer water column and the associated decrease in $CaCO_3$ solubility at higher water temperatures. The latter relationship is apparent in Lake Elsinore via the presence and near absence of $CaCO_3$ during the warmer Holocene versus the colder Glacial, respectively (Kirby et al., 2007, 2013, 2018).

Hydrologically, Lake Elsinore is considered a closed basin lake with only occasional, short-lived overflow (Kirby et al., 2004). Lake level responds directly to the amount of winter precipitation runoff and subsequent summer-to-early fall evaporation (Kirby et al., 2004, 2010). This direct response is not unexpected for arid environment sites, especially those dominated by a winter precipitation climatology such as the PSW (Kirby et al., 2006). Although summer precipitation is a negligible contributor to the lake's annual hydrologic budget, net over-water evaporation peaks in the hot summer-to-early fall months, totaling ~1.4 m evaporation $year^{-1}$ (Anderson, 2001). Simplified, Lake Elsinore's net annual hydrologic budget is a combination of two seasonal end members – winter precipitation (P) and summer-to-early fall evaporation (E), hereafter referred to as the P:E ratio. The winter end member is documented in several papers using changes in grain size and other physical or chemical parameters to infer precipitation-related runoff dynamics (Kirby et al., 2007, 2010, 2013, 2018). However, a direct summer-to-early fall evaporation indicator was not available for Lake Elsinore, thereby limiting our knowledge of Holocene precipitation seasonality trends in the PSW.

## Climatology

The climate of the PSW is Mediterranean – cool, wet winters and hot, dry summers (Bailey, 1966). In general, the coastal plain and low-lying inland regions (i.e., Lake Elsinore) receive less precipitation than the adjacent mountain ranges (Masi, 2005). Year-to year winter precipitation variability is related predominantly to tropical and north Pacific ocean-atmosphere

dynamics and their modulation of the winter storm track over the PSW (Cayan and Peterson, 1989; Brito-Castillo et al., 2003; Hanson et al., 2006). For example, both El Niño-Southern Oscillation (ENSO) and the Pacific Decadal Oscillation (PDO) modulate the mean winter position of the eastern Pacific subtropical high and thus the average latitude of the Pacific winter storm track (Cayan and Peterson, 1989; Brito-Castillo et al., 2003; Hanson et al., 2006). When storms track south, they cause higher than average precipitation and greater river discharge at Lake Elsinore, whereas a more northerly position results in lower than average precipitation and less river discharge (Cayan et al., 1999; Hanson et al., 2006; Gray et al., 2015).

Winter precipitation in the PSW is frequent and characterized by lower precipitation stable oxygen isotope values ($\delta^{18}O_{(precipitation)}$), whereas summer precipitation is infrequent and characterized by higher $\delta^{18}O_{(precipitation)}$ values (Friedman et al., 1992). For example, the average 6-month winter $\delta^{18}O_{(precipitation)}$ value between 1985 and 1986 A.D. for Mt. San Jacinto (the headwaters of Lake Elsinore) was −12.2 and −14.0‰, respectively. Summer $\delta^{18}O_{(precipitation)}$ for the same years averaged −9.2 and −6.9‰. 50 km NNW of Mt. San Jacinto, $\delta^{18}O_{(precipitation)}$ at Big Bear for winter and summer over the same period of time were −11.8, −14.9 and −5.8, −7.1‰, respectively. The contribution of summer precipitation, however, plays no significant role in the annual hydrological budget at Lake Elsinore. Importantly, the Friedman et al. (1992) study confirms that winter precipitation in the PSW is sourced solely from Pacific Ocean-origin storm tracks and that the associated isotopic signature of winter precipitation is significantly lower than summer sourced precipitation.

A study by Williams and Rodoni (1997) focused specifically on the coastal PSW provides a variety of river, groundwater, and lake water $\delta^{18}O$ data. For example, four data points from Lake Elsinore between 1992 and 1994 provide $\delta^{18}O_{(lake\ water)}$ values of +4.00‰ (01/18/92), −5.78‰ (05/28/93), −4.84‰ (09/03/93), and −3.86‰ (01/04/94), respectively. The initial value of +4.00‰ occurred during a period of extreme low lake levels (the second lowest in the 20$^{th}$ century) and its subsequent reflection of a highly evaporative hydrologic system. Following this lowstand is an abrupt increase in lake level caused by several exceptionally wet winters. This period of extreme runoff produced $\delta^{18}O_{(lake\ water)}$ values much lower than anything measured in our study, recording the rapid influx of low $\delta^{18}O$, winter precipitation (Friedman et al., 1992). These studies are important because they reveal the range of $\delta^{18}O_{(lake\ water)}$ values that can occur in arid environment lakes such as Lake Elsinore. As a result, they provide a baseline understanding for the range of potential and measured $\delta^{18}O_{(calcite)}$ values we observe through the Holocene (discussed below).

# MATERIALS AND METHODS

## Core Retrieval and Sedimentology

Details on sediment core LESS02-11 and LEGC03-3 acquisition and sediment methods (i.e., environmental magnetic susceptibility, LOI 550°C, LOI 950°C, and grain size) are detailed in Kirby et al. (2007, 2010). Magnetic susceptibility, LOI 550°C, and LOI 950°C data are included on **Supplementary Table S1**. Grain size data are available on the NOAA Paleoclimatology Data website[1]. New to this paper are x-ray diffraction (XRD) data. Fifty bulk (<2000 μm) sediment samples were analyzed in 2008 using x-ray diffraction at the Institute of Arctic and Alpine Research (University of Colorado, Boulder, CO, United States) to determine their respective mineralogies. The program RockJock (Eberl, 2004) was used to convert the XRD data into mineral type by weight% (e.g., Andrews and Eberl, 2012).

### Age Control

In the absence of salvageable macro- or micro-organic matter, bulk organic matter (i.e., carbon) was used for age control. Eight dates were measured on core LEGC03-2 and 18 dates were measured on LEGC03-3. All radiocarbon samples were measured at the University of California, Irvine W. M. Keck Carbon Cycle Accelerator Mass Spectrometry Laboratory. Each sample was pre-treated with a standard acid-base-acid method. Five ages from LESS02-11 were determined previously by Kirby et al. (2007, 2010), including the surface age (2003 AD, −0.053 kcal BP), Elemental Pb (1975 AD, −0.025 kcal BP), $Cs^{137}$ (1963 AD, −0.013 kcal BP), and exotic pollen markers (*Eucalyptus*, 1910 AD, 0.040 kcal BP; *Erodium*, 1800 AD, 0.15 kcal BP). A new age model was created using the Bacon v.2.2 age-modeling software (Blaauw and Christen, 2011).

## Sediment Isotope Data

Samples were extracted from LEGC03-3 for bulk sediment $\delta^{18}O_{(calcite)}$ and $\delta^{13}C_{(calcite)}$ at approximately 1–3 cm intervals between 10 and 1073 cm ($n$ = 491). Bulk sediment samples were dried at room temperature and gently ground into a powder. Mean (0.5) grain size for the core is 8.4 μm (mode: 10.8 μm), thus suggesting that the $CaCO_3$ component is likely found in the very fine silt size fraction. SEM analyses of lake sediment show distinct micron size $CaCO_3$ grains dispersed throughout the sediment, thus confirming the occurrence of fine grain carbonate (Anderson, 2001). The lack of carbonate bedrock in the lake's drainage basin eliminates the likelihood that the isotopic values record a detrital carbonate source (Engel, 1959). Bulk sediment samples were roasted *in vacuo* at 200°C to remove water and volatile organic contaminants that may confound stable isotope values of carbonate. Stable oxygen and carbon isotope values were obtained using a Finnigan Kiel-IV carbonate preparation device directly coupled to the inlet of a Finnigan MAT 253 ratio mass spectrometer in the stable isotope laboratories at the University of Saskatchewan. Twenty to forty micrograms of carbonate were reacted at 70°C with three drops of anhydrous phosphoric acid for 90 s. Isotope ratios were corrected for acid fractionation and $^{17}O$ contribution and reported in per mil notation (‰) relative to VPDB standards. Precision and calibration of data were monitored through daily analysis of NBS-18 and NBS-19 carbonate standards. $\delta^{18}O$ values of the samples are bracketed by those of the standards. Precision is better than ± 0.1‰ for both carbon and oxygen isotope values.

[1]https://www.ncdc.noaa.gov/data-access/paleoclimatology-data

## Lake Water Data and Oxygen Isotopic Calculations

Lake water isotope samples ($\delta^{18}O$ and $\delta D$) were collected at 0.5 m water depth in the center of the lake throughout the year between January 1, 2006 and April 4, 2010 ($n$ = 72) (**Figure 1**). Each sample was collected using a lake-water rinsed (3x), high density Nalgene 100 mL bottle. Water was filled to the top, immediately covered by parafilm, and the cap tightened firmly. Samples were placed in the cooler and transported to the CSUF Lab where they were stored in a refrigerator (4°C). Water isotope values were measured at either the University of Saskatchewan or the University of Nevada, Las Vegas. At UNLV, waters were analyzed on a ThermoElectron high temperature thermal conversion elemental analyzer (TC/EA) with a ConFlo III interfaced in continuous flow mode to a Delta V Plus mass spectrometer. Samples were injected into a reactor at 1450°C to produce CO and H2 in a stream of ultra-high purity helium, and gasses were separated on a gas chromatograph column. Regular analysis of internal standards was done in each run with unknowns, with standards calibrated to VSMOW and VSLAP, with the latter values defined as −55.5 and −428‰ for $\delta^{18}O$ and $\delta^{2}H$, respectively (Coplen, 1996). At the University of Saskatchewan, water samples were analyzed using a Picarro L1102-i Isotopic Liquid Water Analyzer based on wavelength-scanned cavity ring down spectroscopy (WS-CRDS). Each sample was analyzed six consecutive times. The first three injections were discarded to eliminate memory effects and the averages of the last three injections were used to calculate $\delta^{18}O_{(H2O)}$ and $\delta D_{(H2O)}$ values. No drift calibration was necessary. Long-term sample precision was determined to be ± 0.1‰ for $\delta^{18}O$ and ± 1‰ for $\delta D$ based upon the two internal standards ($n$ = 80). Precision was significantly higher based upon 150 deionized water samples run consecutively ( ± 0.04‰ for $\delta^{18}O$ and ± 0.2‰ for $\delta D$), because the memory effect between the samples was insignificant. δ values ($\delta^{18}O$ and $\delta D$) presented here are in ‰ relative to VSMOW, after calibration to VSMOW-VSLAP. Water temperature was also measured at each water isotope sampling site at 0.5 m water depth throughout the year. Lake level data are from the Elsinore Valley Municipal Water District. We use the Kim and O'Neil (1997) equation to calculate $\delta^{18}O_{(calcite)}$ from the 2006–2010 AD water temperature (°C) and $\delta^{18}O_{(lake\ water)}$ and $\delta D_{(lake\ water)}$ data set.

# RESULTS AND ISOTOPIC INTERPRETATIONS

## Core Sedimentology

LEGC03-3 core description and results for environmental magnetic susceptibility, LOI 550°C, LOI 950°C, and grain size are detailed in Kirby et al. (2007, 2010). Core LEGC03-3 is dominantly a gray, homogenous clayey silt with occasional very-fine-to-fine sand units – most sand units are <1–2 cm thickness and they are often disseminated within matrix. Here, we focus on the calcite, Mg-calcite, and aragonite XRD results, as they are relevant to the isotopic data. Calcite is the dominant carbonate mineral, averaging 6.7 ± 2.9% with a maximum of 15.5% and a minimum of 0.4%. Mg-calcite average 3.0 ± 1.4% with a maximum of 6.2% and a minimum of 0.6%. Aragonite average 0.08 ± 0.13% with a maximum of 0.45% and a minimum of 0.0%. Calcite and Mg-calcite show a positive, but weak correlation ($n$ = 50, $r$ = 0.38, $p$ < 0.006). Aragonite is not correlated to either calcite or Mg-calcite.

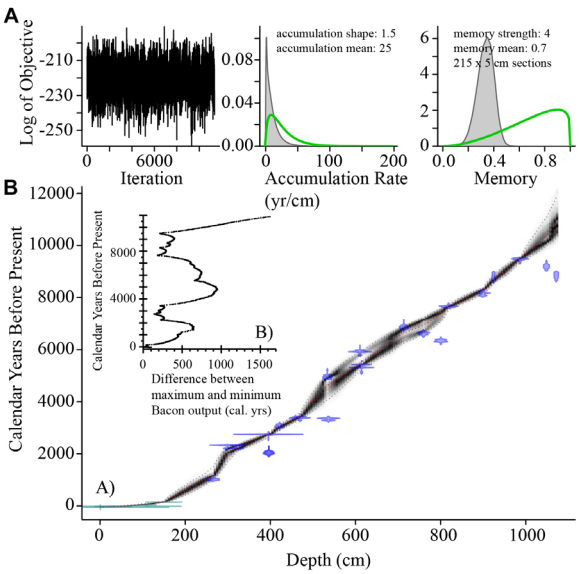


**FIGURE 2 | (A)** Bacon v.2.2 age model for combined LEGC03-3 and LESS02-11 ages. **(B)** Difference between maximum and minimum Bacon v.2.2 age model output. Maximum and minimum based on 2.5 and 97.5% quantiles (95% confidence ranges).

## Age Control

A new age model, building on that from Kirby et al. (2007, 2010), was developed using 26 dates entered into the Bacon v.2.2 (IntCal13) age-modeling software (**Figure 2A** and **Table 1**) (Blaauw and Christen, 2011). Ages from core LESS02-11 and LEGC03-2 were transferred to LEGC03-3 using centimeter-scale sedimentological data to create a single age model for LEGC03-3 spanning −0.053 kcal BP to ∼10.9 kcal BP (Kirby et al., 2010). Five radiocarbon dates were not used in the age model due to suspected reworking (**Table 1**). The date at 105–106 cm is stratigraphically above the *Eucalyptus* pollen age (AD 1910) at 110 cm, and it is therefore considered too old. The dates at 162–163 and 195–196 cm are significantly older than the pollen age at 150 cm. As a result, they require a significant decrease in sedimentation or a hiatus to explain their age-depth relationship. Based on the core description and sedimentological data, we conclude that a sudden decrease in sedimentation and/or a hiatus is unrealistic and requires substantial age model adjustment that is not supported by the sediment data. Finally, the ages at 635–636 and 683–684 cm are from thin, sharply bounded units with higher-than-average magnetic susceptibility and C:N ratios (data not shown), which indicate potential reworking of terrestrial organic matter, thus questioning the accuracy of the bulk organic carbon ages.

**TABLE 1 |** LEGC03-2 and 3 and LESS02-11 age control data.

| Core ID | Depth interval | Core LEGC03-3 equivalent | UCIAMS ID | $\delta^{13}C$ (‰) | $^{14}C$ AGE (BP) | ± | Material dated |
|---|---|---|---|---|---|---|---|
| LESS 02-11ab | 0 | 0 | NA | NA | NA | 0 | Intact Surface (2003 AD) |
| LESS 02-11ab | 31 | 31 | NA | NA | NA | 5 | Elemental Pb (1970 AD) |
| LESS 02-11ab | 46 | 46 | NA | NA | NA | 0 | $^{137}Cs$ (1963 AD) |
| LEGC03-3* | 105–106 | 105.5 | 8263 | −20.7 | 860 | 25 | Bulk organics |
| LESS 02-11ab | 110 | 110 | NA | NA | NA | 10 | Exotic Pollen (*Eucalyptus* ) (1910 AD) |
| LESS 02-11ab | 150 | 150 | NA | NA | NA | 20 | Exotic Pollen (*Erodium* ) (1800 AD) |
| LEGC03-3* | 162–163 | 162.5 | 8264 | −20.4 | 650 | 20 | Bulk organics |
| LEGC03-3* | 195–196 | 195.5 | 8265 | −17.9 | 1,180 | 20 | Bulk organics |
| LEGC03-3 | 264–265 | 264.5 | 8266 | −17.5 | 1,115 | 25 | Bulk organics |
| LEGC03-2 | 298–299 | 299.5 | 8260 | −17.8 | 2,290 | 20 | Bulk organics |
| LEGC03-3 | 324–325 | 324.5 | 8267 | −18.4 | 2,270 | 30 | Bulk organics |
| LEGC03-3 | 395–396 | 395.5 | 8268 | −20.3 | 2,610 | 20 | Bulk organics |
| LEGC03-2 | 405–406 | 396.5 | 6832 | −21.0 | 2,075 | 25 | Bulk organics |
| LEGC03-2 | 405–406 | 396.5 | 6695 | −14.2 | 2,060 | 35 | Bulk organics |
| LEGC03-2 | 432–433 | 421.93 | 8261 | −16.2 | 2,915 | 25 | Bulk organics |
| LEGC03-3 | 469–470 | 469.5 | 8270 | −17.6 | 3,160 | 25 | Bulk organics |
| LEGC03-2 | 556–557 | 533.79 | 8262 | −15.2 | 4,385 | 30 | Bulk organics |
| LEGC03-3 | 536–537 | 536.5 | 8271 | −19.2 | 3,125 | 20 | Bulk organics |
| LEGC03-3 | 610–611 | 610.5 | 8272 | −16.1 | 5,160 | 30 | Bulk organics |
| LEGC03-2 | 624–625 | 614.17 | 6833 | −15.8 | 4,605 | 25 | Bulk organics |
| LEGC03-3* | 635–636 | 635.5 | 8274 | −18.4 | 4,955 | 30 | Bulk organics |
| LEGC03-3* | 683–684 | 683.5 | 8275 | −18.1 | 4,945 | 30 | Bulk organics |
| LEGC03-3 | 713–714 | 713.5 | 8277 | −17.6 | 6,025 | 35 | Bulk organics |
| LEGC03-3 | 759–760 | 759.5 | 8278 | −17.3 | 5,820 | 30 | Bulk organics |
| LEGC03-3 | 800–801 | 800.5 | 8279 | −18.1 | 5,540 | 40 | Bulk organics |
| LEGC03-2 | 850–851 | 818.69 | 6834 | −14.4 | 6,825 | 30 | Bulk organics |
| LEGC03-2 | 947–948 | 899 | 6835 | −17.7 | 7,350 | 30 | Bulk organics |
| LEGC03-3 | 924–925 | 924.5 | 8280 | −19.4 | 7,910 | 50 | Bulk organics |
| LEGC03-3 | 986–987 | 986.5 | 8283 | −14.9 | 8,465 | 40 | Bulk organics |
| LEGC03-3 | 1048–1049 | 1048.5 | 8284 | −17.0 | 8,225 | 40 | Bulk organics |
| LEGC03-3 | 1071–1072 | 1071.5 | 8286 | −18.0 | 7,965 | 40 | Bulk organics |

* = *not used in the age model.*

**Figure 3** illustrates the differences between the Kirby et al. (2007, 2010) age model and that determined for this paper. In general, the difference between the age models increases with depth such that the new Bacon age model is up to 1200 years older at the base of the core than the Kirby et al. (2007, 2010) age model (**Figure 3**). Importantly, this updated age model does not invalidate interpretations in Kirby et al. (2007, 2010). However, the absolute timing of the Kirby et al. (2010) sand-inferred pluvials and droughts have changed (see section "Discussion").

To assess the range of ages associated with the new Bacon age model, we have plotted the difference between the maximum and minimum Bacon age output on **Figure 2B**. The maximum and minimum ages represent the 95% confidence ranges, based on 2.5 and 97.5% quantiles (Blaauw and Christen, 2011). This assessment shows that the age range is greatest between 0.5 and 2.0 kcal BP (up to 680 years), 4.0–7.0 kcal BP (up to a 1000 years), and 9.8 kcal BP through to the core bottom (up to 1600 years). Knowing this range of ages provides some constraint of the accuracy of the assigned pluvial and drought intervals. Considering this range of potential ages, we limit our temporal interpretation to centennial-to-multi-centennial timescales to account for age model uncertainty. Future use of these sand and isotope data should consider this inherent age variability when interpreting apparent site-to-site correlations.

## Modern Lake Water and Sediment Isotope Comparisons

Recent lake level and lake water isotopic data are shown in **Figure 4**. For the period of overlapping data, lake level ranges from a minimum of 377.6 m to a maximum of 381.2 m. Over the same period, $\delta^{18}O_{(lake\ water)}$ ranges from a minimum of −1.0‰ to a maximum of 5.3‰ ($n$ = 72) with a mean of 2.4‰ (**Supplementary Table S2**). $\delta D_{(lake\ water)}$ ranges from a minimum of −19.2‰ to a maximum of 12.1‰ ($n$ = 72) with a mean value of −2.3‰ (**Supplementary Table S2**). Notably, there is a negative relationship between lake level and $\delta^{18}O_{(lake\ water)}$ between 1/3/2006 and 4/2/2010. As lake level drops, the $\delta^{18}O_{(lake\ water)}$ values increase (**Figure 4**). This coupling is expected in an arid environment where

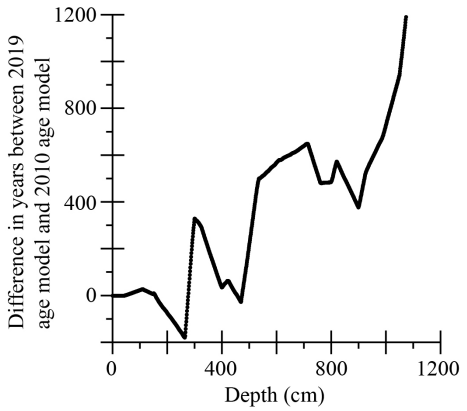


**FIGURE 3 |** Difference in years (cal BP) between the 2019 Elsinore Bacon v.2.2 age model and the Kirby et al. (2010) age model.

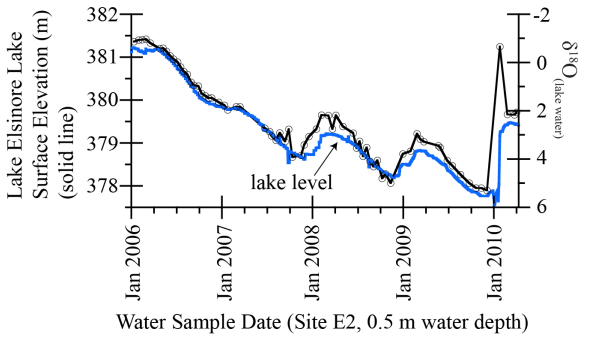


**FIGURE 4 |** Lake Elsinore lake level (m) and measured lake water (0.5 m water depth) $\delta^{18}O$ values.

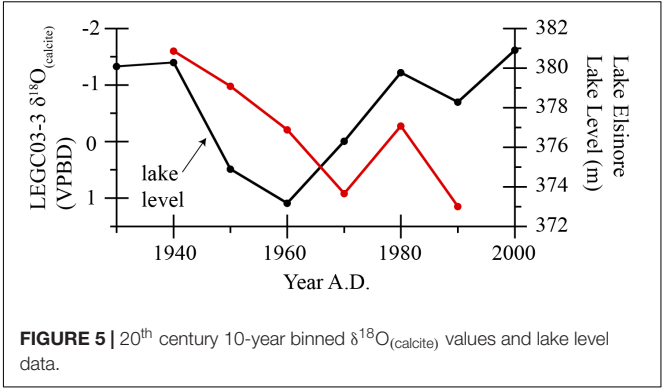


**FIGURE 5 |** 20th century 10-year binned $\delta^{18}O_{(calcite)}$ values and lake level data.

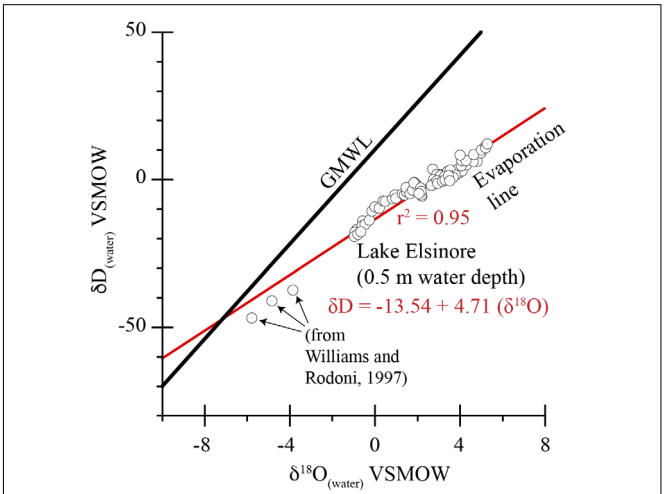


**FIGURE 6 |** Lake Elsinore water (0.5 m water depth) oxygen and hydrogen isotopic values plotted versus the GMWL. Note the strong departure from the GMWL by the Lake Elsinore $\delta^{18}O_{(lake\ water)}$ values in response to evaporation.

annual net evaporation strongly influences lake hydrology (Leng and Marshall, 2004; Dean et al., 2015; Anderson et al., 2016). As an additional test of this modern relationship, we compare 20th century 10-year binned Lake Elsinore lake level to core LEGC03-3 $\delta^{18}O_{(calcite)}$ data (**Figure 5**). A similar negative relationship is observed; although, the 20th century comparison is based on only six data points. Other factors that may have influenced the 20th century relationship include: (1) human modification of the influent during and following the 1950s drought (Hudson, 1978), which likely altered natural $\delta^{18}O_{(lake\ water)}$ values; and (2) high uncertainty associated with the 20th century age model (**Figure 2** and **Table 1**). Nonetheless, both the modern and 20th century data suggest that changes in $\delta^{18}O_{(lake\ water)}$ values reflect the relative strength of over-water evaporation and its modulation of the lake's hydrologic and isotopic budget. Finally, a strong departure from the Global Meteoric Water Line (GMWL) further supports the interpretation that evaporation plays a dominant role in governing the lake's isotopic composition (**Figure 6**) (Williams and Rodoni, 1997).

Lake water temperatures measured at the same location and depth (0.5 m below the lake surface) as the water isotope samples, range from a minimum of 9.4°C to a maximum of 28.9°C with a mean of 20.3°C ($n$ = 77) (**Figure 7** and **Supplementary Table S2**). These temperature data are combined with the measured $\delta^{18}O_{(lake\ water)}$ values to calculate the $\delta^{18}O_{(calc\ sed\ calcite)}$ values using the Kim and O'Neil (1997) equation. These calculations were made to examine how well the modern system captures the range of $\delta^{18}O_{(calcite)}$ values observed in the Holocene (**Figure 8**), and to evaluate if the modern system a reasonable benchmark for interpreting the paleo $\delta^{18}O_{(calcite)}$ values. The similarity between calculated modern (range = −3 to 5‰) and Holocene (range = −7.9 to 5.1‰) values suggests that our modern $\delta^{18}O_{(calc\ sed\ calcite)}$ values capture a large part of the natural isotopic variability in the Lake Elsinore system and are congruent with values measured in the paleo-record (**Figures 7**, **8**). This indicates that fractionation between $\delta^{18}O_{(lake\ water)}$ and subsequent epilimnic $\delta^{18}O_{(calcite)}$ values is likely conservative and reflects similar drivers through time. Time-averaging the Holocene $\delta^{18}O_{(calcite)}$ values into 100-year bins dampens higher frequency isotopic variability and their effect on our interpretations, such as that caused by potential non-equilibrium processes, changes in over-water

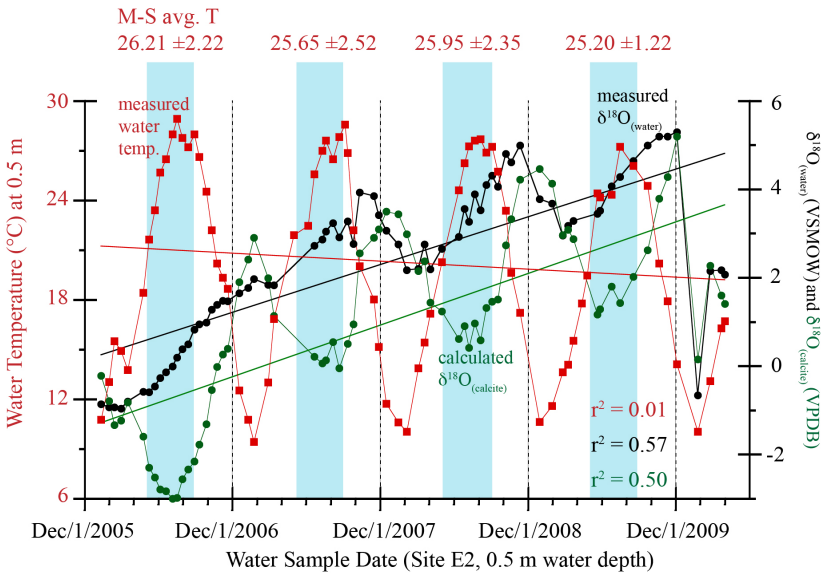


**FIGURE 7 |** Lake Elsinore measured $\delta^{18}O_{(lake\ water)}$ values, measured water temperature (0.5 m water depth), and $\delta^{18}O_{(calc.sed.calcite)}$. Shaded areas represent months of peak calcite precipitation. Average May (M) – September (S) lake water temperatures are shown at the top of the figure with standard deviation values.

relative humidity, and/or other unforeseen isotopic imbalances (Gat, 1996; Leng and Marshall, 2004).

Calculated $\delta^{18}O_{(calc\ sed\ calcite)}$ values range from a minimum of −3.0‰ to a maximum of 5.2‰ with a mean of 1.0‰ ($n = 72$) (**Figure 7**). Whilst lake temperatures show no significant trend over the period of study, the $\delta^{18}O_{(lake\ water)}$ and the $\delta^{18}O_{(calc\ sed\ calcite)}$ data show a very similar 4+ year trend. Over the 4+ years of measured data, lake level dropped consistently with only nominal winter recovery (**Figure 4**). Lake water isotopic values capture this evaporative trend as do the calculated $\delta^{18}O_{(calc\ sed\ calcite)}$ values. The combination of, and relationship between, measured lake level data, measured $\delta^{18}O_{(lake\ water)}$ values, and $\delta^{18}O_{(calc\ sed\ calcite)}$ values provides the basis for our interpretation that the predominant control on Lake Elsinore sediment $\delta^{18}O_{(calcite)}$ values over time is the isotopic value of the lake water, not water temperature. As additional support for this interpretation, we note that predominant interval of epilimnic calcite precipitation is likely during the late spring through early fall, when lake productivity re-emerges from its winter dormancy (or suppression) (**Figure 7**). During this period of peak calcite precipitation, lake water temperatures – averaged from May through September – are relatively stable and uniformly warm from year-to-year, thus contributing nominally to the resultant $\delta^{18}O_{(calcite)}$ values (Anderson, 2001) (**Figure 7**).

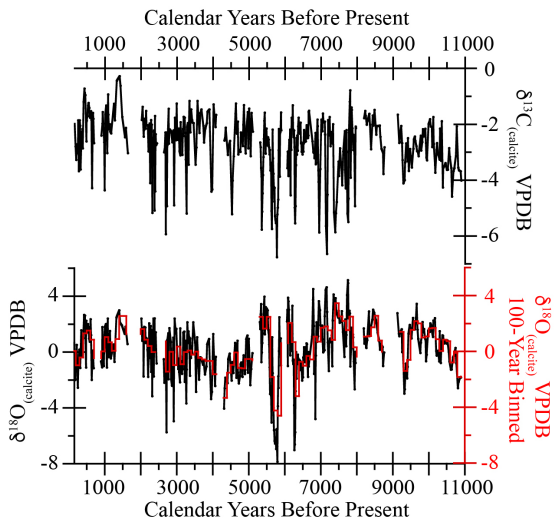


**FIGURE 8 |** Raw bulk sediment $\delta^{18}O_{(calcite)}$ and $\delta^{13}C_{(calcite)}$ values. The solid red line represent the 100-year binned $\delta^{18}O_{(calcite)}$ data.

## Holocene Sediment Oxygen Isotope Data

The raw and 100-year binned sediment isotope data are shown by **Figure 8**. Although the raw data are shown, the discussion is based on $\delta^{18}O_{(calcite)}$ 100-year binned averages to account for age model uncertainty (e.g., 0.2 kcal BP BIN = 0.15–0.25 kcal BP average value, etc.) (**Figure 8** and **Supplementary Table S3**). Centuries not included in the binned data due to either missing core or disturbed sections include: 0.8, 1.7–1.9, 2.5, 4.2, 5.2, 6.0, 8.1, and 8.8–9.1 kcal BP. Intervals not included due to too few data points for an accurate 100-year bin include: 0–1.0, 1.5, 2.6, 3.9, and 4.1–4.3 kcal BP. The raw $\delta^{18}O_{(calcite)}$ range from a minimum of −7.9‰ to a maximum of 5.1‰ VPDB with a mean 0.2‰ and a standard deviation of 2.1‰ ($n = 491$) (**Figure 8**). Notably, the Holocene range of $\delta^{18}O_{(calcite)}$ values as well as the mean are not too dissimilar to the $\delta^{18}O_{(calc\ sed\ calcite)}$ values (**Figure 7**), excepting the anomalously low $\delta^{18}O_{(calcite)}$ values ca. 5.7–5.8 kcal BP. We interpret this similarity to indicate that our 4+ year modern study captured a fair amount of the natural variation – in terms of averages and max/min – that

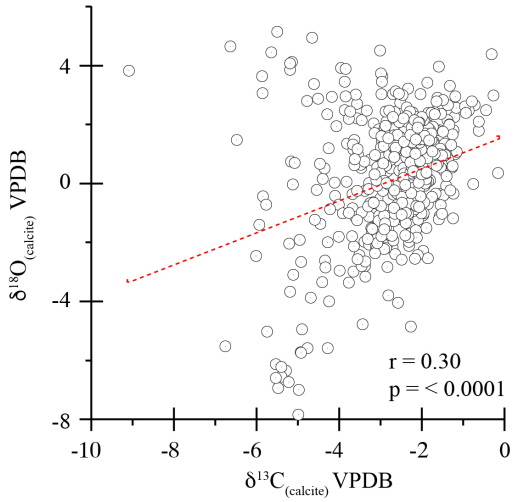


**FIGURE 9 |** Scatter plot comparing Holocene sediment $\delta^{18}O_{(calcite)}$ and $\delta^{13}C_{(calcite)}$ values.

occur at Lake Elsinore. $\delta^{18}O_{(calcite)}$ show a weak, but positive correlation to both LOI 550°C ($r = 0.23$, $p < 0.0001$, $n = 491$) and LOI 950°C ($r = 0.21$, $p < 0.0001$, $n = 491$). $\delta^{13}C_{(calcite)}$ range from a minimum of −9.1‰ to a maximum of −0.2‰ with a mean of −2.7‰ and a standard deviation of 1.2‰ ($n = 491$) (**Figure 5** and **Supplementary Table S4**). $\delta^{18}O_{(calcite)}$ to $\delta^{13}C_{(calcite)}$ covariance over the length of the record is poor ($r = 0.30$) but statistically significant ($p = < 0.001$), possibly indicating sustained periods of lake closure, $\delta^{13}C_{(DIC)}$ evaporative enrichment, and/or a productivity link related to seasonal evapoconcentration of nutrients, or a transition in terrestrial supply of DIC, DOC, and POC associated with decreased precipitation (**Figure 9**) (Talbot, 1990; Drummond et al., 1995; Li and Ku, 1997; Kirby et al., 2002; Leng and Marshall, 2004; Horton et al., 2016). A more detailed look at $\delta^{18}O_{(calcite)}$ to $\delta^{13}C_{(calcite)}$ covariance reveals six intervals of positive and statistically significant covariance, and one interval of negative and statistically significant covariance (**Supplementary Table S5**). This detailed examination of $\delta^{18}O_{(calcite)}$ to $\delta^{13}C_{(calcite)}$ covariance suggests a predominantly closed basin through time, as suspected based on 20th century lake level data (**Figures 4**, **5**) (Kirby et al., 2004). The $\delta^{13}C_{(calcite)}$ Holocene data are not discussed further here.

The relationship between the 100-year binned $\delta^{18}O_{(calcite)}$ values and the 100-year binned sand data is not statistically significant ($n = 90$, $r = -0.02$, $p < 0.84$), indicting that there is no *consistent* relationship between $\delta^{18}O_{(calcite)}$ values (i.e., E in the P:E relationship) and the sand data (i.e., P in the P:E relationship) over the Holocene. In the discussion we explore the relationship between the $\delta^{18}O_{(calcite)}$ values and the sand data on a century-to-century basis to identify intervals of similar or dissimilar responses. Based on this comparison, we infer the duration and severity of Holocene droughts and pluvials as well as speculate on a generalized Holocene lake level interpretation for Lake Elsinore.

# DISCUSSION

## Holocene Pluvials, Droughts, and Lake Level

Using the similarity between the Holocene and 20th century average $\delta^{18}O_{(calcite)}$ values (0.2 and −0.3‰, respectively), we select 0.0‰ as the break point to define above-average and below-average, Holocene summer-to-early fall over-water evaporation (**Figure 10**). These 100-year binned data are then bracketed by color (orange = above-average evaporation; blue = below-average evaporation), when there are two or more adjacent 100-year bins.

At first look, the $\delta^{18}O_{(calcite)}$ data can be divided into three millennial scale intervals characterizing changes in summer-to-early fall, over-water evaporation: (1) the highly evaporative Early Holocene (10.45–6.65 kcal BP), (2) the less evaporative Mid-Holocene (6.65–2.65 kcal BP); and (3) the evaporative Late Holocene (2.65–0.55 kcal BP) (**Figure 7**). As an independent assessment of the $\delta^{18}O_{(calcite)}$ data from core LEGC03-3, we compare to $\delta^{18}O_{(calcite)}$ values from a separately dated sediment core extracted from the lake's modern littoral zone (LESS02-5; Kirby et al., 2004) (**Figures 1**, **10**). Although not perfect, the comparison exhibits similar changes across the interval of shared time (3.5–1.8 kcal BP), suggesting that our profundal core reliably records the lake's integrated isotopic signal.

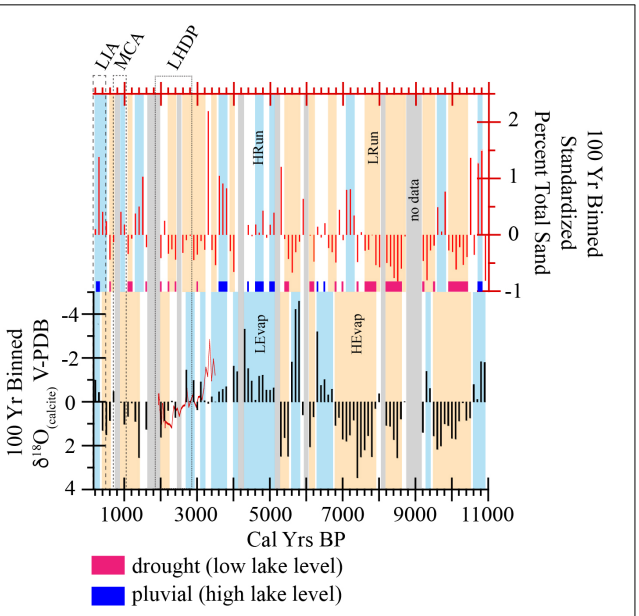


**FIGURE 10 |** 100-year binned $\delta^{18}O_{(calcite)}$ and sand values. Inset line on the bottom graph shows the $\delta^{18}O_{(calcite)}$ data from LESS02-5 (Kirby et al., 2004) on its own age model. The light blue and light orange boxes unique to each data set reflect intervals of two or more centuries of above/below-average $\delta^{18}O_{(calcite)}$ or sand. Intervals of shared $\delta^{18}O_{(calcite)}$ values and sand drought are shown by dark red boxes and vice versa for pluvials (dark blue boxes) at the intersection of the upper and lower graphs. HRun, high runoff; LRun, low runoff; LEvap, low evaporation; HEvap, high evaporation; LIA, Little Ice Age (Masson-Delmotte et al., 2013); MCA, Medieval Climatic Anomaly (Masson-Delmotte et al., 2013); Late Holocene Dry Period (Mensing et al., 2013).

Changes in lake water $\delta^{18}O$ values from which the calcite precipitates reflect both evaporation during the peak season of calcitic mineralization as well as changes in the relative influx of low $\delta^{18}O$, winter precipitation runoff. As a result, the final interpretation of the $\delta^{18}O_{(calcite)}$ values must consider the latter. To assess the role played by winter season precipitation (P) and its relative input of low $\delta^{18}O$ runoff, the $\delta^{18}O_{(calcite)}$ data were compared to the Kirby et al. (2010) sand-inferred winter precipitation runoff data; these data are similarly binned by 100-years and colored coded. Despite the poor statistical relationship between the two variables ($n$ = 90, $r$ = −0.02, $p$ < 0.84), comparison between the individual 100-year bins provides insight to centuries sharing a similar signal (e.g., low sand [less winter precipitation runoff] plus high $\delta^{18}O_{(calcite)}$ [evaporative summers] = drought [low lake level] and vice versa for pluvials). Drought are colored coded as red and pluvials as dark blue (**Figure 10**). **Supplementary Table S3** provides a list of inferred drought (low lake level) and pluvial (high lake level) centuries, based on this visual comparison.

Taken together, this comparison reveals a dynamic Holocene hydroclimate characterized by centennial to multi-centennial scale intervals of both above-average and below-average winter precipitation (pluvials) and summer-to-early fall over-water evaporation (drought) (**Figure 10** and **Supplementary Table S3**). In general, the same three-part millennial scale Holocene divisions are observed as described above. However, our P:E comparison (i.e., sand vs. $\delta^{18}O_{(calcite)}$) informs on the duration and severity of centennial to multi-centennial scale wet-dry periods that are not apparent when examining only the $\delta^{18}O_{(calcite)}$ or sand data. Long-lasting droughts, indicated by low lake levels, occurred in the Early Holocene (10.45–5.35 kcal BP). There is only one sustained pluvial during this time (10.85–10.65 kcal BP). By 5.15 kcal BP, there is shift to more frequent pluvials ($n$ = 9 centuries [periods of high lake level]) until 3.55 kcal BP, with the longest between 4.85 and 4.55 kcal BP. From 3.05 to 0.55 kcal BP, there are eight centennial droughts (periods of low lake level) with no apparent pluvials. The most recent, pre-historical (>0.15 kcal BP) pluvial occurs during the Little Ice Age (0.35–0.15 kcal BP). We note that there are several intervals that lack data (unrecovered core sections or disturbed sediment or too few data points for an accurate 100-year bin; **Supplementary Table S3**).

To assess the $\delta^{18}O_{(calcite)}$ evaporation interpretation, we use the only existing, quantitative reconstruction of Holocene summer temperature from the PSW (Wahl, 2003; Ohlwein and Wahl, 2012). This pollen-based, July temperature anomaly reconstruction was derived using a 253 cm sediment core from a wet meadow (Taquitz Meadow, 33°46′8″ N, 116°39′44″ W, 2399 m elevation) in the San Jacinto Mountains (**Figure 11**) (Wahl, 2003; Ohlwein and Wahl, 2012). Temperature anomalies were reconstructed using a "Bayesian generalized linear model based on pollen ratios of (all conifers)/(all conifers + oak + important shrubs)" (Ohlwein and Wahl, 2012). Limitations of this temperature reconstruction are likely associated with a "systematic underestimation of model uncertainties due to a spatial correlation of unaccounted explanatory variables" (Ohlwein and Wahl, 2012). The reconstruction is temporally-constrained using

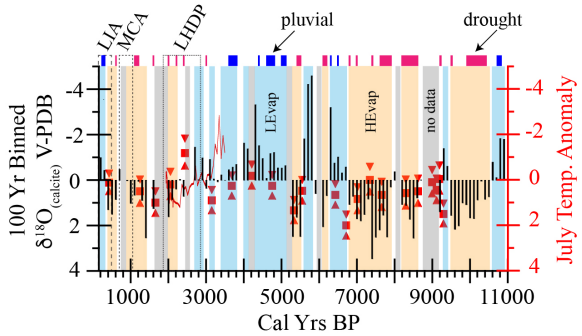


**FIGURE 11 |** 100-year binned $\delta^{18}O_{(calcite)}$ values versus the pollen July temperature anomaly reconstruction (July temperature axis is inverted) from the San Jacinto Mountains (Wahl, 2003; Ohlwein and Wahl, 2012). Inverted triangles represent the one-sigma range associated with the temperature reconstruction (Wahl, 2003; Ohlwein and Wahl, 2012). Intervals of shared $\delta^{18}O_{(calcite)}$ values and sand drought are shown by dark red boxes and vice versa for pluvials (dark blue boxes) at the graph. LEvap, low evaporation; HEvap, high evaporation; LIA, Little Ice Age (Masson-Delmotte et al., 2013); MCA, Medieval Climatic Anomaly (Masson-Delmotte et al., 2013); Late Holocene Dry Period (Mensing et al., 2013).

an age-to-age linear sedimentation rate age model based on eight radiocarbon dates between 30 and 243 cm (Wahl, 2002). The surface age is assumed the year the core was recovered. Each sample represents about 20–50 years integrated time. Notably, there is a thick event layer between 124 and 151 cm depth, which is interpreted to reflect a single storm event in the catchment (Wahl, 2002). The reconstruction uses only one sample from this event layer. Using the Bacon v.2.2 age-modeling software (Blaauw and Christen, 2011), we explored how different and up-dated age models – without removing the event layer – influenced the timing of the reconstruction. Our analyses revealed no significant difference between Wahl's (2002) age-to-age linear sedimentation rate age model and our Bacon v.2.2 derived age model. As a result, we use Wahl's (2002) age model for comparison to our isotope data (**Figure 11**).

In general, the pollen-based, July temperature anomaly reconstruction shows average-to-above-average July temperatures for most of Holocene, with approximately 4°C one-sigma total temperature range. A closer look at longer trends reveals a more nuanced signal (**Figure 11**; July temperature axis is inverted). However, to avoid over-interpretation, and with consideration for the differences in sample-to-sample resolution between the Elsinore and the Taquitz Meadow records, we limit our comparison to the three Elsinore $\delta^{18}O_{(calcite)}$-derived Holocene intervals: (1) the highly evaporative Early Holocene (10.55–6.65 kcal BP), (2) the less evaporative Mid-Holocene (6.65–2.65 kcal BP); and (3) the evaporative Late Holocene (2.65–0.55 kcal BP) (**Figure 7**). Early Holocene July temperature anomalies are characterized by average-to-above average temperatures with limited variability (Ohlwein and Wahl, 2012). The Mid-Holocene, however, reveals a general trend toward lower July temperatures, reaching a low at 4.2 kcal BP, before rising slightly until 3.1 kcal BP. This Mid Holocene

interval is also characterized by the largest amplitude, Holocene temperature changes reconstructed. Finally, the Late Holocene begins with the largest negative July temperature anomaly on record at 2.4 kcal BP. Following this negative excursion, temperatures rise and stabilize at or slightly below average.

The millennial scale trends are broadly similar but it is important to recognize the limitations of the comparison. For example, the $\delta^{18}O_{(calcite)}$ data are scale independent such that any given isotopic value cannot be assigned an absolute value for evaporation rate. Furthermore, ecological inertia limits the functional response of the vegetation to environmental stresses. The hydrology of Lake Elsinore, however, experiences change on a variety of timescales (**Figures 4**, **5**, **8**), that are unlikely recorded in the San Jacinto pollen-temperature record (Kirby et al., 2018).

## CONCLUSION

Although the PSW's hydroclimate is dominated by winter precipitation, summer evaporation (i.e., temperature) plays an important role in lake and reservoir hydrology. This input–output dynamic is often referred to the as the P:E ratio for lakes in arid and semi-arid environments. Lake Elsinore is a good site for evaluating the interplay between winter precipitation, summer evaporation, and lake hydrology. Until now, the story told using Lake Elsinore sediments has been winter focused. Kirby et al. (2010) inferred wet-dry intervals over the past 9.7 kcal BP, using changes in sand content to interpret winter-related, paleo-runoff.

In the PSW, drought is often contributed to deficits in winter precipitation only. However, the most recent Californian drought (2012–2015 AD) highlighted the importance of temperature as an amplifier of drought conditions (Griffin and Anchukaitis, 2014; Diffenbaugh et al., 2015; Shukla et al., 2015; Luo et al., 2017). This temperature-related drought is now referred to as a "hot drought" (Griffin and Anchukaitis, 2014; Diffenbaugh et al., 2015; Shukla et al., 2015; Luo et al., 2017). In the PSW, summer-to-early fall temperatures coincide with maximum evaporation and subsequent lake level regressions (**Figure 4**). Coupled with less winter precipitation, a hot drought can produce large changes in a lake's hydrologic budget – larger perhaps than winter precipitation deficits alone. To examine the relative roles of winter precipitation and summer-to-early fall evaporation (i.e., temperature) in the geological record requires seasonally-sensitive indicators. Knowing this, we coupled the Kirby et al. (2010) winter precipitation, runoff indicator (i.e., sand) with $\delta^{18}O_{(calcite)}$ values – a well-known recorder of evaporation in arid and semi-arid lacustrine environments. We also updated the age model using a more sophisticated Bayesian methodology.

Together, these data reveal periods of sustained drought (i.e., lower lake levels) based on 100-year bins of shared high $\delta^{18}O_{(calcite)}$ values (i.e., greater summer-to-early fall over-water evaporation) and low sand content (lower winter precipitation runoff). The opposite relationship is used to infer pluvials. In general, the Early Holocene is characterized by the driest summers (high $\delta^{18}O_{(calcite)}$ values) and the lowest winter precipitation runoff (low sand content). The Mid-Holocene sees a return to more mild conditions with lower over-water evaporation and several pluvial episodes. Evaporative conditions and associated drought return in the Late Holocene with the exception of the wet LIA.

Finally, from a broader North Pacific point of view, Lake Elsinore is located far south of the average latitude (∼40°N latitude) of the western United States winter precipitation dipole (Dettinger et al., 1998; Wise, 2010, 2016). As a result, the lake represents a key location for comparison to sites located within, and north of, the dipole. Future work will examine the spatial expression, strength, and persistence of the precipitation dipole during the Holocene. However, our results suggest that – when possible – researchers should locate and study sediment records that capture some component of seasonality, to view a more nuanced view of past climate. This nuanced view is required if we are to understand the relative roles played by changes in seasonality as well as to examine/evaluate the forcings that modulate Holocene drought and pluvials.

## AUTHOR CONTRIBUTIONS

MK conceived the project, interpreted the data, and wrote the manuscript. WP produced the sediment isotope data and some of the water isotope data, reviewed and edited the manuscript. ML produced some of the water isotope data, reviewed and edited the manuscript. JN collected the water samples, reviewed and edited the manuscript. MA collected some of the water samples, reviewed and edited the manuscript. KN helped with the Bacon age model. JA reviewed and edited the manuscript.

## FUNDING

This research was funded by the National Science Foundation (EAR-0602269-01) to MK. Additional funds were provided by a Lake Elsinore-San Jacinto Water Authority (LESJWA) contract to MK and MA and the American Chemical Society-Petroleum Research Fund (ACS-PRF: Grant #41789-GB8) to MK. Funds from Cal-State Fullerton Faculty-Student Creative Research Grants provided summer stipends for several students.

## ACKNOWLEDGMENTS

Special thanks to the City of Lake Elsinore, particularly Mr. Patrick Kilroy (former Lake Manager) for access to the lake; Mr. David Ruhl (LESJWA) for contract management; Gregg Drilling and Testing, Inc. for exceptional quality service. Thanks to Dr. Sandra Timsic whom analyzed water and calcite samples in the Saskatchewan Isotope Lab. We thank three reviewers as well as LA for thorough, insightful, and helpful comments.

## SUPPLEMENTARY MATERIAL

The Supplementary Material for this article can be found online at: https://www.frontiersin.org/articles/10.3389/feart.2019.00074/full#supplementary-material

## REFERENCES


Anderson, L., Berkelhammer, M., Barron, J. A., Steinman, B. A., Finney, B. P., Abbott, M. B., et al. (2016). Lake oxygen isotopes as recorders of North American Rocky mountain hydroclimate: holocene patterns and variability at multi-decadal to millennial time scales. *Global Planet. Change* 137, 131–148. doi: 10.1016/j.gloplacha.2015.12.021

Anderson, M. A. (2001). *Internal Loading and Nutrient Cycling in Lake Elsinore*. Lake Elsinore: Santa Ana Regional Water Quality Control Board, 52.

Anderson, R. Y., Hemphill-Haley, E., and Gardner, J. V. (1987). Persistent late pleistocene-holocene seasonal upwelling and varves off the coast of California. *Quat. Res.* 28, 307–313. doi: 10.1016/0033-5894(87)90069-X

Anderson, W. T., Mullins, H. T., and Ito, E. (1997). Stable isotope record from Seneca Lake, New York: evidence for a cold paleoclimate following the Younger Dryas. *Geology* 25, 135–138. doi: 10.1130/0091-7613(1997)025<0135:SIRFSL>2.3.CO;2

Andrews, J. T., and Eberl, D. D. (2012). Determination of sediment provenance by unmixing the mineralogy of source-area sediments: the "SedUnMix" program. *Mar. Geol.* 29, 24–33. doi: 10.1016/j.margeo.2011.10.007

Ault, T. R., Cole, J. E., Overpeck, J. T., Pederson, G. T., St George, S., Otto-Bliesner, B., et al. (2013). The continuum of hydroclimate variability in western north america during the last millennium. *J. Clim.* 26, 5863–5878. doi: 10.1175/JCLI-D-11-00732.1

Bailey, H. P. (1966). *The Climate of Southern*. Berkeley, CA: University of California Press.

Benson, L., Kashgarian, M., Rye, R., Lund, S., Paillet, F., Smoot, J., et al. (2002). Holocene multidecadal and multicentennial droughts affecting Northern California and Nevada. *Quat. Sci. Rev.* 21, 659–682. doi: 10.1016/S0277-3791(01)00048-8

Bird, B. W., and Kirby, M. E. (2006). An alpine lacustrine record of early Holocene North American Monsoon dynamics from Dry Lake, southern California (USA). *J. Paleolimnol.* 35, 179–192. doi: 10.1007/s10933-005-8514-3

Bird, B. W., Kirby, M. E., Howat, I. M., and Tulaczyk, S. (2010). Geophysical evidence for Holocene lake-level change in southern California (Dry Lake). *Boreas* 39, 131–144. doi: 10.1111/j.1502-3885.2009.00114.x

Blaauw, M., and Christen, J. A. (2011). Flexible paleoclimate age-depth models using an autoregressive gamma process. *Bayesian Anal.* 6, 457–474.

Brito-Castillo, L., Douglas, A. V., Leyva-Contreras, A., and Lluch-Belda, D. (2003). The effect of large-scale circulation on precipitation and streamflow in the Gulf of California continental watershed. *Int. J. Climatol.* 23, 751–768. doi: 10.1002/joc.913

Cayan, D. R., and Peterson, D. H. (1989). "The influence of North Pacific atmospheric circulation on streamflow in the west," in *Aspects of Climate Variability in the Pacific and the Western Americas*, Vol. 55, ed. D. H. Peterson (Washington, DC: American Geophysical Union), 375–397.

Cayan, D. R., Redmond, K. T., and Riddle, R. G. (1999). ENSO and hydrologic extremes in the western United States. *J. Climate* 12, 2881–2893. doi: 10.1175/1520-0442(1999)012<2881:EAHEIT>2.0.CO;2

Cook, B. I., Ault, T. R., and Smerdon, J. E. (2015). Unprecedented 21st century drought risk in the American Southwest and Central Plains. *Sci. Adv.* 1:e1400082. doi: 10.1126/sciadv.1400082

Cook, B. I., Smerdon, J. E., Seager, R., and Cook, E. R. (2014). Pan-continental droughts in North America over the Last Millennium. *J. Clim.* 27, 383–397. doi: 10.1175/JCLI-D-13-00100.1

Cook, E. R., Seager, R., Cane, M. A., and Stahle, D. W. (2007). North American drought: reconstructions, causes, and consequences. *Earth-Sci. Rev.* 81, 93–134. doi: 10.1016/j.earscirev.2006.12.002

Coplen, T. B. (1996). New guidelines for reporting stable hydrogen, carbon, and oxygen isotope-ratio data. *Geochim. Cosmochim. Acta* 60, 3359–3360. doi: 10.1016/0016-7037(96)00263-3

Dean, J. R., Eastwood, W. J., Roberts, N., Jones, M. D., Yiğitbaşıoğlu, H., Allcock, S. L., et al. (2015). Tracking the hydro-climatic signal from lake to sediment: a field study from central Turkey. *J. Hydrol.* 529, 608–621. doi: 10.1016/j.jhydrol.2014.11.004

Dettinger, M. D., Cayan, D. R., Diaz, H. F., and Meko, D. M. (1998). North-south precipitation patterns in western North America on interannual-to-decadal timescales. *J. Clim.* 11, 3095–3111. doi: 10.1175/1520-0442(1998)011<3095:NSPPIW>2.0.CO;2

Diffenbaugh, N. S., Swain, D. L., and Touma, D. (2015). Anthropogenic warming has increased drought risk in California. *Proc. Natl. Acad. Sci. U.S.A.* 112, 3931–3936. doi: 10.1073/pnas.1422385112

Drummond, C. N., Patterson, W. P., and Walker, J. C. (1995). Climatic forcing of carbon-oxygen isotopic covariance in temperate-region marl lakes. *Geology* 23, 1031–1034. doi: 10.1130/0091-7613(1995)023<1031:CFOCOI>2.3.CO;2

Eberl, D. (2004). Quantitative mineralogy of the Yukon River system: changes with reach and season, and determining sediment provenance. *Am. Mineral.* 89, 1784–1794. doi: 10.2138/am-2004-11-1225

Engel, R. (1959). *Geology of the Lake Elsinore Quadrangle, California*. San Francisco, CA: California Division of Mines, 52.

Enzel, Y., and Wells, S. G. (1997). Extracting Holocene paleohydrology and paleoclimatology information from modern extreme flood events: an example from southern California. *Geomorphology* 19, 203–226. doi: 10.1016/S0169-555X(97)00015-9

Friedman, I., Smith, G. I., Gleason, J. D., Warden, A., and Harris, J. M. (1992). Stable isotope composition of waters in Southeastern California.1. Modern Precipitation. *J. Geophys. Res. Atmos.* 97, 5795–5812. doi: 10.1029/92JD00184

Gat, J. R. (1996). Oxygen and hydrogen isotopes in the hydrologic cycle. *Anu. Rev. Earth Planet. Sci.* 24, 225–262. doi: 10.1146/annurev.earth.24.1.225

Graumlich, L. J. (1993). A 1000-year record of temperature and precipitation in the sierra-nevada. *Quat. Res.* 39, 249–255. doi: 10.1006/qres.1993.1029

Gray, A. B., Pasternack, G. B., Watson, E. B., Warrick, J. A., and Goñi, M. A. (2015). The effect of El Niño Southern Oscillation cycles on the decadal scale suspended sediment behavior of a coastal dry-summer subtropical catchment. *Earth Surf. Process. Landforms* 40, 272–284. doi: 10.1002/esp.3627

Griffin, D., and Anchukaitis, K. J. (2014). How unusual is the 2012-2014 California drought? *Geophys. Res. Lett.* 41, 9017–9023. doi: 10.1002/2014GL062433

Hanson, R. T., Dettinger, M. D., and Newhouse, M. W. (2006). Relations between climatic variability and hydrologic time series from four alluvial basins across the southwestern United States. *Hydrogeol. J.* 14, 1122–1146. doi: 10.1007/s10040-006-0067-7

Hodell, D. A., Schelske, C. L., Fahnenstiel, G. L., and Robbins, L. L. (1998). Biologically induced calcite and its isotopic composition in Lake Ontario. *Limnol. Oceanogr.* 43, 187–199. doi: 10.4319/lo.1998.43.2.0187

Holmgren, C. A., Betancourt, J. L., and Rylander, K. A. (2010). A long-term vegetation history of the Mojave-Colorado desert ecotone at Joshua Tree National Park. *J. Quat. Sci.* 25, 222–236. doi: 10.1002/jqs.1313

Horton, T. W., Defliese, W. F., Tripati, A. K., and Oze, C. (2016). Evaporation induced 18 O and 13 C enrichment in lake systems: a global perspective on hydrologic balance effects. *Quat. Sci. Rev.* 131, 365–379. doi: 10.1016/j.quascirev.2015.06.030

Hudson, T. (1978). *Lake Elsinore Valley: Its Story*, 3rd Edn. Lake Elsinore, CA: Mayhall Print Shop.

Hughes, M. K., and Graumlich, L. J. (1996). "Climatic variations and forcing mechanisms of the last 2000 years," in *Multi-Millennial Dendroclimatic Studies from the Western United States*, eds P. D. Jones, R. S. Bradley, J. Jouzel (Berlin: Springer), 109–124. doi: 10.1007/978-3-642-61113-1_6

Hull, A. G. (1990). Seismotectonics of the Northern Elsinore fault zone, southern California. *Bull. Seismol. Soc. Am.* 82, 800–818.

Kelts, K., and Talbot, M. R. (1990). "Lacustrine carbonates as geochemical archives of environmental change and biotic/abiotic interactions," in *Large Lakes: Ecological Structure and Function*, Chap. 15, eds M. M. Tilzer and C. Serruya. (Berlin: Springer-Verlag), 288–315.

Kim, S.-T., and O'Neil, J. R. (1997). Equilibrium and nonequilibrium oxygen isotope effects in synthetic carbonates. *Geochim. Cosmochim. Acta* 61, 3461–3475. doi: 10.1016/S0016-7037(97)00169-5

Kirby, M. E., Feakins, S. J., Bonuso, N., Fantozzi, J. M., and Hiner, C. A. (2013). Latest pleistocene to Holocene hydroclimates from Lake Elsinore, California. *Quat. Sci. Rev.* 76, 1–15. doi: 10.1016/j.quascirev.2013.05.023

Kirby, M. E., Feakins, S. J., Hiner, C. A., Fantozzi, J., Zimmerman, S. R. H., Dingemans, T., et al. (2014). Tropical pacific forcing of Late-Holocene hydrologic variability in the coastal southwest United States. *Quat. Sci. Rev.* 102, 27–38. doi: 10.1016/j.quascirev.2014.08.005

Kirby, M. E., Heusser, L., Scholz, C., Ramezan, R., Anderson, M. A., Markle, B., et al. (2018). A late Wisconsin (32-10k cal a BP) history of pluvials, droughts and

vegetation in the pacific south-west United States (Lake Elsinore, CA). *J. Quat. Sci.* 33, 238–254. doi: 10.1002/jqs.3018

Kirby, M. E., Knell, E. J., Anderson, W. T., Lachniet, M. S., Palermo, J., Eeg, H., et al. (2015). Evidence for insolation and Pacific forcing of late glacial through Holocene climate in the Central Mojave Desert (Silver Lake, CA). *Quat. Res.* 84, 174–186. doi: 10.1016/j.yqres.2015.07.003

Kirby, M. E., Lund, S. P., Anderson, M. A., and Bird, B. W. (2007). Insolation forcing of Holocene climate change in Southern California: a sediment study from Lake Elsinore. *J. Paleolimnol.* 38, 395–417. doi: 10.1007/s10933-006-9085-7

Kirby, M. E., Lund, S. P., and Bird, B. W. (2006). Mid-Wisconsin sediment record from Baldwin Lake reveals hemispheric climate dynamics (Southern CA, USA). *Palaeogeogr. Palaeoclimatol. Palaeoecol.* 241, 267–283. doi: 10.1016/j.palaeo.2006.03.043

Kirby, M. E., Lund, S. P., Patterson, W. P., Anderson, M. A., Bird, B. W., Ivanovici, L., et al. (2010). A Holocene record of pacific decadal oscillation (PDO)-related hydrologic variability in Southern California (Lake Elsinore, CA). *J. Paleolimnol.* 44, 819–839. doi: 10.1007/s10933-010-9454-0

Kirby, M. E., Lund, S. P., and Poulsen, C. J. (2005). Hydrologic variability and the onset of modern El Nino Southern Oscillation: a 19,250-year record from Lake Elsinore, southern California. *J. Quat. Sci.* 20, 239–254. doi: 10.1002/jqs.906

Kirby, M. E., Mullins, H. T., Patterson, W. P., and Burnett, A. W. (2002). Late glacial-Holocene atmospheric circulation and precipitation in the northeast United States inferred from modern calibrated stable oxygen and carbon isotopes. *Geol. Soc. Am. Bull.* 114, 1326–1340. doi: 10.1130/0016-7606(2002)114<1326:LGHACA>2.0.CO;2

Kirby, M. E., Poulsen, C. J., Lund, S. P., Patterson, W. P., Reidy, L., Hammond, D. E., et al. (2004). Late Holocene lake level dynamics inferred from magnetic susceptibility and stable oxygen isotope data: Lake Elsinore, southern California (USA). *J. Paleolimnol.* 31, 275–293. doi: 10.1023/B:JOPL.0000021710.39800.f6

Kirby, M. E., Zimmerman, S. R. H., Patterson, W. P., and Rivera, J. J. (2012). A 9170-year record of decadal-to-multi-centennial scale pluvial episodes from the coastal Southwest United States: a role for atmospheric rivers? *Quat. Sci. Rev.* 46, 57–65. doi: 10.1016/j.quascirev.2012.05.008

Labotka, D., Grissino-Mayer, H., Mora, C., and Johnson, E. (2016). Patterns of moisture source and climate variability in the southeastern United States: a four-century seasonally resolved tree-ring oxygen-isotope record. *Clim. Dynam.* 46, 2145–2154. doi: 10.1007/s00382-015-2694-y

Lajewski, C., Mullins, H., Patterson, W., and Callinan, C. (2003). Historic calcite record from the Finger Lakes, New York: impact of acid rain on a buffered terrane. *Geol. Soc. Am. Bull.* 115, 373–384. doi: 10.1130/0016-7606(2003)115<0373:HCRFTF>2.0.CO;2

Leavitt, S. W., and Long, A. (1991). Seasonal stable-carbon isotope variability in tree rings: possible paleoenvironmental signals. *Chem. Geol. Isotope Geosci. Sect.* 87, 59–70. doi: 10.1016/0168-9622(91)90033-S

Lebo, M. E., Reuter, J. E., and Meyers, P. A. (1994). Historical changes in sediments of Pyramid Lake, Nevada, USA: consequences of changes in the water balance of a terminal desert lake. *J. Paleolimnol.* 12, 87–101. doi: 10.1007/BF00678089

Leng, M. J., and Marshall, J. D. (2004). Palaeoclimate interpretation of stable isotope data from lake sediment archives. *Quat. Sci. Rev.* 23, 811–831. doi: 10.1016/j.quascirev.2003.06.012

Li, H. C., Bischoff, J. L., Ku, T. L., Lund, S. P., and Stott, L. D. (2000). Climate variability in east-central California during the past 1000 years reflected by high-resolution geochemical and isotopic records from Owens Lake sediments. *Quat. Res.* 54, 189–197. doi: 10.1006/qres.2000.2163

Li, H.-C., and Ku, T.-L. (1997). delta13C-delta18O covariance as a paleohydrological indicator for closed-basin lakes. *Palaeogeogr. Palaeoclimatol. Palaeoecol.* 133, 69–80. doi: 10.1016/S0031-0182(96)00153-8

Luo, L., Apps, D., Arcand, S., Xu, H., Pan, M., Hoerling, M., et al. (2017). Contribution of temperature and precipitation anomalies to the California drought during 2012–2015. *Geophys. Res. Lett.* 44, 3184–3192. doi: 10.1002/2016GL072027

Masi, G. J. (2005). "Orographic and large-scale influence on Southern California precipitation patterns," in *Proceedings of the Sixth Conference on Coastal Atmospheric and Oceanic Prediction and Processes*, San Diego, CA.

Masson-Delmotte, V., Schulz, M., Abe-Ouchi, A., Beer, J., Ganopolski, A., Gonzaìlez Rouco, J. F., et al. (2013). "Information from paleoclimate archives," in *Climate Change 2013: The Physical Science Basis. Contribution of Working Group I to the Fifth Assessment Report of the Intergovernmental Panel on Climate Change*, eds T. F. Stocker, D. Qin, G.-K. Plattner, M. Tignor, S. K. Allen, J. Boschung, et al. (Cambridge: Cambridge University Press), 383–464.

McDonald, E. V., McFadden, L. D., Wells, S. G., Enzel, Y., and Lancaster, N. (2003). "Regional response of alluvial fans to the pleistocene-holocene climatic transition, Mojave Desert, California," in *Paleoenvironments and Paleohydrology of the Mojave and Southern Great Basin Deserts*, eds Y. Enzel, S. G. Wells, and N. Lancaster (Boulder, CO: Geological Society of America Special Paper) 368, 189–205. doi: 10.1130/0-8137-2368-X.189

Meko, D. M., Therrell, M. D., Baisan, C. H., and Hughes, M. K. (2001). Sacramento river flow reconstructed to A.D. 869 from tree Rings1. *JAWRA J. Am. Water Resour. Assoc.* 37, 1029–1039. doi: 10.1111/j.1752-1688.2001.tb05530.x

Mensing, S. A., Sharpe, S. E., Tunno, I., Sada, D. W., Thomas, J. M., Starratt, S., et al. (2013). The late holocene dry period: multiproxy evidence for an extended drought between 2800 and 1850 cal yr BP across the central Great Basin, USA. *Quat. Sci. Rev.* 78, 266–282. doi: 10.1016/j.quascirev.2013.08.010

Metcalfe, S. E., Barron, J. A., and Davies, S. J. (2015). The Holocene history of the North American Monsoon: 'known knowns' and 'known unknowns' in understanding its spatial and temporal complexity. *Quat. Sci. Rev.* 120, 1–27. doi: 10.1016/j.quascirev.2015.04.004

Miller, D. M., Schmidt, K. M., Mahan, S. A., McGeehin, J. P., Owen, L. A., Barron, J. A., et al. (2010). Holocene landscape response to seasonality of storms in the Mojave Desert. *Quat. Int.* 215, 45–61. doi: 10.1016/j.quaint.2009.10.001

Mullins, H. T. (1998). Environmental change controls of lacustrine carbonate, Cayuga Lake, New York. *Geology* 26, 443–446. doi: 10.1130/0091-7613(1998)026<0443:ECCOLC>2.3.CO;2

Mullins, H. T., Patterson, W. P., Teece, M. A., and Burnett, A. W. (2011). Holocene climate and environmental change in central New York (USA). *J. Paleolimnol.* 45, 243–256. doi: 10.1007/s10933-011-9495-z

Ohlwein, C., and Wahl, E. R. (2012). Review of probabilistic pollen-climate transfer methods. *Quat. Sci. Rev.* 31, 17–29. doi: 10.1016/j.quascirev.2011.11.002

Pigati, J. S., Miller, D. M., Bright, J. E., Mahan, S. A., Nekola, J. C., Paces, J. B., et al. (2011). Chronology, sedimentology, and microfauna of groundwater discharge deposits in the central Mojave Desert, Valley Wells, California. *Geol. Soc. Am. Bull.* 123, 2224–2239. doi: 10.1130/B30357.1

Shukla, S., Safeeq, M., AghaKouchak, A., Guan, K., and Funk, C. (2015). Temperature impacts on the water year 2014 drought in California. *Geophys. Res. Lett.* 42, 4384–4393. doi: 10.1002/2015GL063666

St George, S., and Ault, T. R. (2014). The imprint of climate within Northern Hemisphere trees. *Quat. Sci. Rev.* 89, 1–4. doi: 10.1016/j.quascirev.2014.01.007

Steinman, B. A., and Abbott, M. B. (2013). Isotopic and hydrologic responses of small, closed lakes to climate variability: hydroclimate reconstructions from lake sediment oxygen isotope records and mass balance models. *Geochim. Cosmochim. Acta* 105, 342–359. doi: 10.1016/j.gca.2012.11.027

Stuiver, M. (1970). Oxygen and carbon isotope ratios of fresh-water carbonates as climatic indicator. *J. Geophys. Res.* 75, 5247–5257. doi: 10.1029/JC075i027p05247

Talbot, M. R. (1990). A review of the palaeohydrological interpretation of carbon and oxygen isotopic ratios in primary lacustrine carbonates. *Chem. Geol. (Isotope Geosci. Sect.)* 80, 261–279. doi: 10.1016/0168-9622(90)90009-2

Thompson, J. B., SchultzeLam, S., Beveridge, T. J., and DesMarais, D. J. (1997). Whiting events: biogenic origin due to the photosynthetic activity of cyanobacterial picoplankton. *Limnol. Oceanogr.* 42, 133–141. doi: 10.4319/lo.1997.42.1.0133

Wahl, E. R. (2002). *Paleoecology and Testing of Paleoclimate Hypotheses in Southern California During the Holocene*. PhD Dissertation, University of Minnesota, Minneapolis, MN, 248.

Wahl, E. R. (2003). Assigning climate values to modern pollen surface sample sites and validating modern analog climate reconstructions in the southern California region. *Madroño* 50, 271–285.

Wells, S. G., Brown, J. B., Enzel, Y., Anderson, R. Y., and McFadden, L. D. (2003). "Late quaternary geology and paleohydrology of pluvial Lake Mojave, southern California," in *Paleoenvironments and Paleohydrology of the Mojave and Southern Great Basin Deserts*, eds Y. Enzel, S. G. Wells, and N. Lancaster

(Boulder, CO: Geological Society of America), 79–115. doi: 10.1130/0-8137-2368-X.79

Williams, A. E., and Rodoni, D. P. (1997). Regional isotope effects and application to hydrologic investigations in southwestern California. *Water Resour. Res.* 33, 1721–1729. doi: 10.1029/97WR01035

Wise, E. K. (2010). Spatiotemporal variability of the precipitation dipole transition zone in the western United States. *Geophys. Res. Lett.* 37, L07706. doi: 10.1029/2009GL042193

Wise, E. K. (2016). Five centuries of US West Coast drought: occurrence, spatial distribution, and associated atmospheric circulation patterns. *Geophys. Res. Lett.* 43, 4539–4546. doi: 10.1002/2016GL068487

Wurster, C. M., and Patterson, W. P. (2001). Seasonal variation in stable oxygen and carbon isotope values recovered from modern lacustrine freshwater mollusks: paleoclimatological implications for sub-weekly temperature records. *J. Paleolimnol.* 26, 205–218. doi: 10.1023/A:1011194011250

**Conflict of Interest Statement:** The authors declare that the research was conducted in the absence of any commercial or financial relationships that could be construed as a potential conflict of interest.